The Automatic Quantification of Morphological Features of Pectus Excavatum Based on Three-Dimensional Images

Nadine A. Coorens, MSc,[,†,‡,1] Jean H.T. Daemen, MD,[*,‡,1] Cornelis H. Slump, MSc, PhD,[†] Tom G.J. Loonen, MSc,[§] Yvonne L.J. Vissers, MD, PhD,[*] Karel W.E. Hulsewé, MD, PhD,[*] and Erik R. de Loos, MD[*]*

Visual examination and quantification of severity are essential for clinical decision making in patients with pectus excavatum. Yet, visual assessment is prone to inter- and intra-observer variability and current quantitative methods are inadequate. This study aims to develop and evaluate a novel, automatic and non-invasive method to objectively quantify pectus excavatum morphology based on three-dimensional images. Key steps of the automatic analysis are normalization of image orientation, slicing, and computation of the morphological features encompassing pectus depth, width, length, volume, position, steepness, flaring, asymmetry and mean cross-sectional area. A digital phantom mimicking a patient with pectus excavatum was used to verify the analysis method. Prospective three-dimensional imaging and subsequent surface analysis in patients with pectus excavatum was performed to assess clinical feasibility. Verification of the developed analysis tool demonstrated 100% reproducibility of all morphological feature values. Calculated parameters compared to the predetermined phantom dimensions were accurate for all but four features. The pectus width, length, volume and steepness showed an error of 4 mm (4%), 2 mm (2%), 12 mL (5%) and 1 degree (3%), respectively. Prospective imaging of 52 patients (88% males) demonstrated the feasibility of the developed tool to quantify morphological features of pectus excavatum in the clinical setting. Mean duration to calculate all features in one patient was 7.6 seconds. We have developed and presented a non-invasive pectus excavatum surface analysis tool, that is feasible to automatically quantify morphological features based on three-dimensional images with promising accuracy and reproducibility.

Semin Thoracic Surg ■■:■■–■■

Keywords: Pectus excavatum, Pectus excavatum surface morphology, Inter- and intra-observer variability, Three-dimensional optical surface imaging, Surface analysis

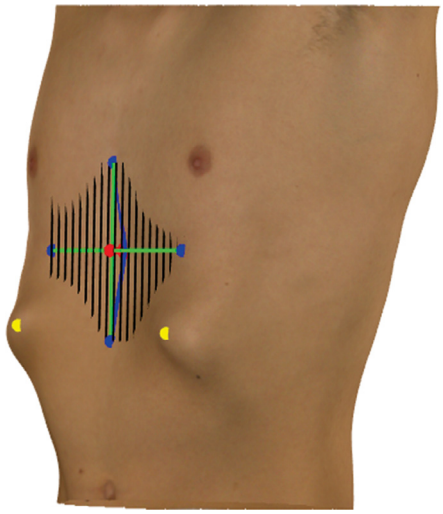

Three-dimensional surface analysis of morphologic features of pectus excavatum.

Central Message

We have developed, verified and prospectively evaluated an innovative and non-invasive surface analysis tool that automatically quantifies morphologic features of pectus excavatum using 3D images.

Perspective Statement

The automatic quantification of morphological features allows for an objective and non-

Abbreviations: 3D, three-dimensional; IQR, interquartile range

*Department of Surgery, Division of General Thoracic Surgery, Zuyderland Medical Center, Heerlen, The Netherlands
[†]Faculty of Science and Technology (S&T), University of Twente, Enschede, The Netherlands
[‡]Faculty of Health, Medicine and Life Sciences (FHML), School for Oncology and Developmental Biology (GROW), Maastricht, The Netherlands
[§]3D Lab Radboudumc, Radboud University Medical Center, Nijmegen, The Netherlands

Funding: This work was supported by the Zuyderland Research and Innovation Fund of Zuyderland Medical Center (Heerlen, the Netherlands) [grant number 2019-005].

Conflicts of Interest: None of the authors had any conflicts to declare.

[1]Equal contribution status

Address reprint requests to Erik R. de Loos, MD, Department of Surgery, Division of General Thoracic Surgery; Zuyderland Medical Center; Henri Dunantstraat 5, 6419PC, Heerlen, The Netherlands. E-mail: e.deloos@zuyderland.nl

1043-0679/$–see front matter

https://doi.org/10.1053/j.semtcvs.2021.05.018

INTRODUCTION

Pectus excavatum accounts for up to 90% of all chest wall deformities[1] with a birth prevalence of 1 in 400.[2] In essence, pectus excavatum is characterized by a posterior depression of the sternum. However, multiple other features contribute to its presentation, including sternal rotation (leading to asymmetry), flaring (ie, anterior protrusion of the inferior costal arch), and the position and extent of depression.[1,3] The combination and degree of these features define the patient-specific clinical presentation of pectus excavatum. Attempts to qualitatively describe and characterize variations in pectus morphology have led to the utilization of descriptive subtypes, for example trench-, saucer- and cup-shaped types.[4,5] Unfortunately, this qualitative classification is inherently related to inter-observer and intra-observer variability,[6] in contrast to a more objective quantitative assessment.

To date, a variety of indices have been proposed to quantify pectus excavatum. Among these indices, the Haller index is still considered as the gold standard[7] to determine surgical candidacy. However, as stressed by Martinez-Ferro, none of the current measures are without limitations.[7] For instance, the Haller index depends on thoracic shape, vertebral level at which it is measured, age and sex, and it does not consider asymmetry, nor other morphological features. Hence, it may fail to comprehensively assess the deformity, emphasizing the need for alternative methods to quantify pectus excavatum.[7] As suggested, the perfect index might be a mathematical combination of different aspects of pectus excavatum.[7]

Based on these conclusions, we propose that a new approach should be able to reflect the full three-dimensional extent of the deformity. An automatic assessment tool based on 3D images of the chest may provide objective quantification and documentation of the morphological characteristics of pectus excavatum. Since this approach has not been studied to date, the research question of this study was: is it feasible to objectively and automatically quantify the three-dimensional morphology of pectus excavatum based on non-invasive 3D images?

MATERIALS AND METHODS

To answer this research question, the study was divided into three stages: (1) development of an automated surface analysis tool to evaluate 3D images of pectus excavatum patients, (2) verification of this developed tool and (3) assessment of its clinical feasibility through prospective acquisition of 3D images and analysis in patients with pectus excavatum.

Development of the surface analysis tool was based on three-dimensional surface images acquired using a handheld Artec Leo imaging system (Artec3D, Luxembourg, Luxembourg). This is a structured light scanner that projects a grid pattern on the subject and captures the distortion in stereoscopic vision. The disparity between images is used to calculate depth information though triangulation, thereby creating a digital 3D mesh of the scanned surface. The device uses a built-in accelerometer, gyroscope and compass to monitor its position during scanning and does not require additional markers for tracking.

invasive assessment of pectus excavatum, eliminating inter- and intra-observer variability. Three-dimensional features may form the basis for comprehensive severity classification, prediction of aesthetic outcome and individualized planning of surgical treatment.

Development of Surface Analysis Tool

The essential features of pectus excavatum to be identified and computed by the surface analysis tool were determined after assessment of the available literature and consultation of two experienced general thoracic surgeons (YV, EdL). The selected features include the pectus excavatum depth, width, length, volume, position (ie, point of onset and maximum depth), steepness, flaring, asymmetry and mean cross-sectional area.[5,8] The surface analysis tool was developed using MATLAB (MATLAB R2019a, The Mathworks Inc., Natick, MA, USA), which is a programming platform enabling computations on three-dimensional geometries (eg triangulated surfaces) generated by the imaging device.

Pre-Processing Phase

Prior to the quantification of features, pre-processing of 3D images is required and encompasses normalization of the image orientation, selection of the region of interest and slicing of the 3D images. The method of pre-processing has partially been adapted from Glinkowksi et al.[9] The following sections describe the pre-processing phase in more detail.

Normalization of orientation. Normalization through alignment of the 3D image and system axes facilitates standardization of measurements obtained along specific axes. Since the Artec Leo device is able to automatically align the floor with the transversal plane, only a rotational correction of the longitudinal axis is required. An optimal correction is defined as the state wherein the transversal torso width is maximal. The tool calculates and selects the median correction angle of all transversal image slices to correct the longitudinal axis (see Fig. 1A).

Selection of region of interest. To focus on the thoracic area which is generally affected by pectus excavatum, a region of interest is defined within the three-dimensional image. To account for differences in height between patients, the region of interest is based on a set of ratios. The cranial 1/8th and caudal 1/4th portions of the 3D image are disregarded, leaving a region of interest with a length of 5/8th of the original 3D image length (see Fig. 1B).

Slicing of the 3D images. After alignment of the axes, the 3D image is divided in transversal (Fig. 1C) and sagittal (Fig. 1D) slices with a fixed thickness of 2 mm. This slice thickness was chosen to prevent voids in the surface (ie elements without vertices), because the density of vertices may vary between areas. Intersection of every transversal and sagittal slice results in a 2-by-2 mm bar-shaped element which height equals the distance

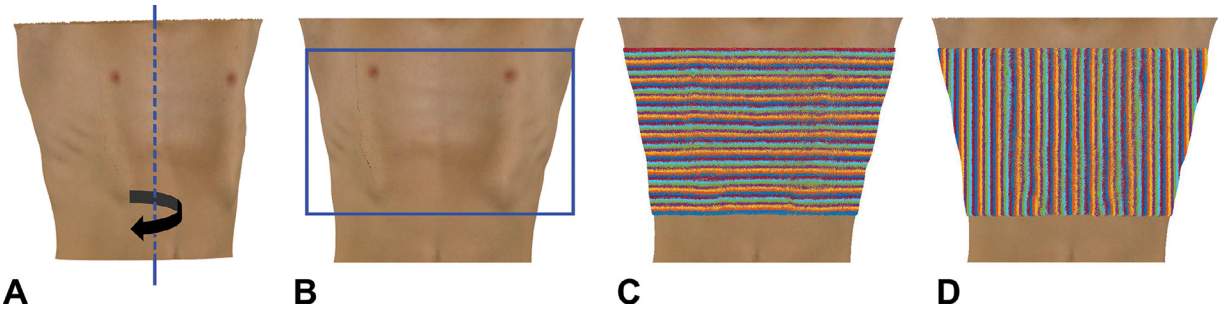

Figure 1. Pre-processing phases of three-dimensional images of patients with pectus excavatum. (A) Images are automatically rotated along the longitudinal body axis (dashed blue line) to obtain a normalized orientation. (B) A region of interest (blue box) is defined that is cranially and caudally bounded by approximate levels of the sternomanubrial junction and transverse costal plane, respectively. The image is sliced with 2 mm thickness in the (C) transversal and (D) sagittal direction (Color version of figure is available online at http://www.semthorcardiovascsurg.com).

between the mean heights of the anterior and posterior surface vertices in that element. These elements are used in the quantification of all pectus excavatum features.

Quantification of Surface Features

Pectus depth. The point of maximum thoracic depression is identified in two stages. First, a preliminary point is identified that servers as an auxiliary for the actual point. The preliminary point is the location of maximum depression in between bilateral maxima of the anterior chest per transversal slice (see Fig. 2A). The actual point is situated at the largest distance (pectus depth) between the anterior chest surface and craniocaudal surface line plotted from the cranial to caudal maxima along the identical sagittal slice exhibiting the preliminary point (see Fig. 2B). This step is required to cope with the cranial thoracic surface that is often posteriorly angulated and being misidentified as deepest point. This especially counts for mild pectus excavatum. The pectus depth corresponds with the largest distance with respect to the craniocaudal reference line. This facilitates comparability between males and females, since breast formation may overestimate the pectus depth when a transversal reference is used.

Pectus position. Two pectus positions are defined: the cranial onset point of the depression and location of the most excavated point with respect to the suprasternal notch. The onset is defined as the most cranial point where the inward depression initiates and automatically identified by the tool. The positions are expressed as percentage, with a value closer to 0% when the point is located more cranially (0% = at the suprasternal notch) and closer to 100% when the point is located more caudally (100% = at the umbilicus). See the example from Figure 2C.

Pectus steepness. Steepness of the depression is determined in four directions (Figure 2D). Utilizing the point of maximum posterior displacement as origin, the angle between the coronal plane and cranial, caudal, right lateral and left lateral most anterior surface point is calculated. The angles serve as a measure of steepness.

Pectus width and length. The size of the depression is expressed by its width and length. The width is defined as the Euclidean distance between the bilateral most anterior surface points used for steepness calculations. Similarly, the length is defined as the Euclidean distance between the cranial and caudal surface points.

Flaring. Flaring is defined as anterior protrusion of the costal arch and is located below the transverse midline of the torso. The flaring height is quantified by the perpendicular distance between the flaring point and medial most posterior surface point (see Fig. 2E).

Pectus volume. The pectus volume describes the volume of the external depression in milliliters. A rectangular plane is placed over the excavation, of which the sides are bordered by the most cranial, caudal, right lateral and left lateral most anterior surface point utilized for steepness calculation. The volume is estimated by the content between the body surface and plane (see Fig. 2F).

Asymmetry. Asymmetry was based on relative volumetric differences. The 3D image is divided in a left- and right hemithorax by the mid-sagittal slice. Asymmetry is calculated for the entire 3D image, but also for the single transversal slice encompassing the deepest point that, respectively, identifies global and localized asymmetry. The level of asymmetry is expressed as percentage where a negative value indicates a lower volume of the left hemithorax.

Mean cross-sectional area. The mean cross-sectional area of the thorax can be used in the clinical setting to emphasize or nuance other characteristics. For example, a large compared to small mean cross-sectional area, both with the same depth, depicts a less severe pectus excavatum. The mean cross-sectional area is computed by dividing the total thoracic volume by its length (within the region of interest).

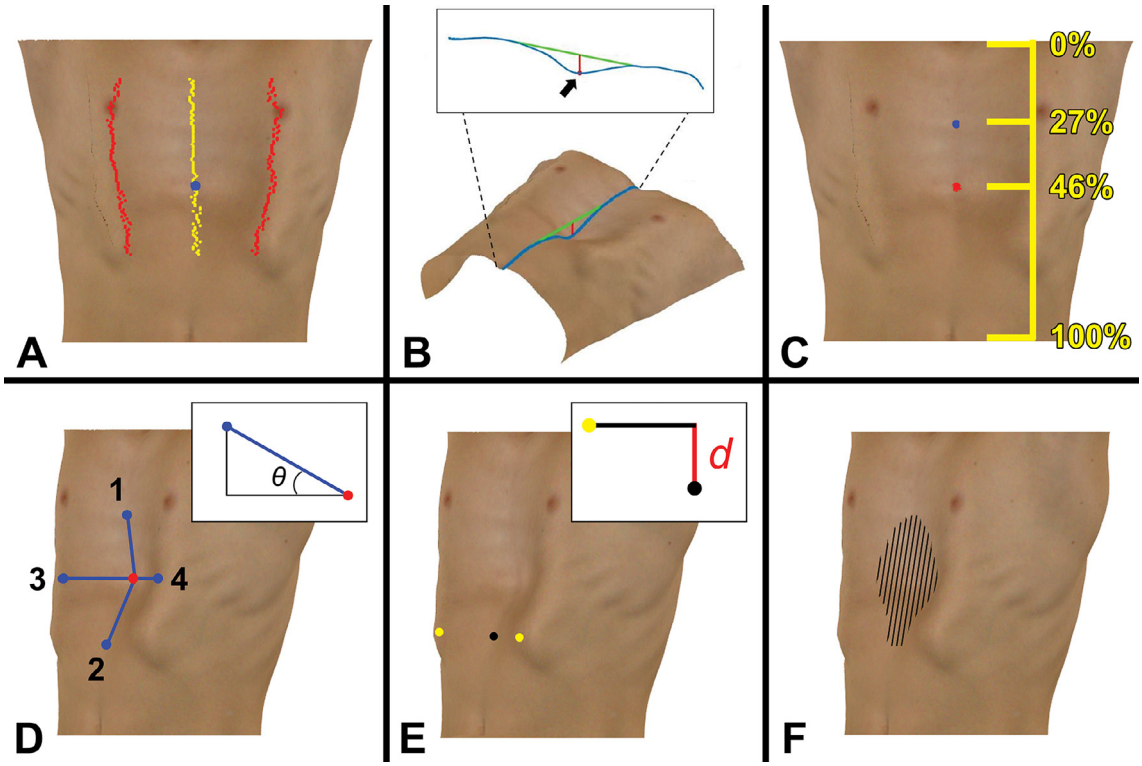

Figure 2. Quantification of morphological features of pectus excavatum. (A) The automatic identification of the bilateral maxima (red), central minima (yellow) and overall minimum (blue; ie, preliminary point of maximum depression) serves as an auxiliary in the process of finding the actual pectus point. (B) The actual pectus point (black arrow) is situated at the largest distance (red) between the anterior chest surface (blue) and craniocaudal surface line (green) along the sagittal slice defined by the preliminary point. The largest distance (red) corresponds to the pectus depth. (C) The position of the cranial onset of the depression (blue dot) and point of maximum depression (red dot), depicted as percentage of the torso length. (D) The pectus steepness (θ) in the cranial (1), caudal (2) and right (3) and left (4) lateral direction (blue lines) with the actual pectus point (red) as origin. (E) Flaring quantified by the perpendicular distance between the flaring point (yellow) and medial most posterior surface point (black) in the same transversal slice. (F) Quantification of the pectus volume, defined as the volume between the image chest surface and an approximation of the reconstructed chest wall surface (black striped area) (Color version of figure is available online at http://www.semthorcardiovascsurg.com).

Verification of the Analysis Tool

After development of the tool, verification was performed through assessment of the accuracy and reproducibility of computed pectus excavatum characteristics. A digital phantom that mimicks a male patient with a cup-shaped pectus excavatum (See Fig. 3A) was utilized for verification. The phantom was created in-silico using MATLAB and defined by a 3D point cloud of an elliptic cylinder with a longitudinal, maximum transversal and maximum antero-posterior length of 340 mm, 310 mm and 210 mm, respectively. To simulate the inward deformity, a hemispherical depression (radius: 50 mm; equals depth) was created anteriorly with its center in the mid-sagittal plane at a distance of 140 mm to the cranial end. Flaring was simulated by bilateral protruding hemispheres with a radius of 20 mm. To assess reproducibility of both the normalization and feature quantification, the phantom was in fivefold subjected to the analysis tool in various orientations around its longitudinal axis. Calculated values were tested against the ground truth features of the digital phantom to assess validity of the tool.

Prospective Imaging and Analysis

Prospective imaging was performed to assess clinical feasibility of the automated feature quantification by the developed surface analysis tool. All outpatients consulted for pectus excavatum at Zuyderland Medical Center (Heerlen, the Netherlands) between August 2019 and August 2020 were prospectively imaged and retrospectively analyzed. Patients with any form of light-hypersensitivity (eg, photosensitive epilepsy) were excluded due to the use of light flashes during 3D image acquisition. In addition, patients with prior surgical correction and patients with clearly no thoracic depression were excluded. The study was approved by the local ethical committee for scientific research (METC Zuyderland, ID: METCZ20190048, date of approval: April 19, 2019). Written informed consent was obtained from all participants. Additional consent was obtained from the patient's parent(s) or legal guardian if younger than 16 years of age.

All participants underwent 3D imaging of their pectus excavatum using the handheld Artec Leo imaging system (Artec3D, Luxembourg, Luxembourg) according to the protocol

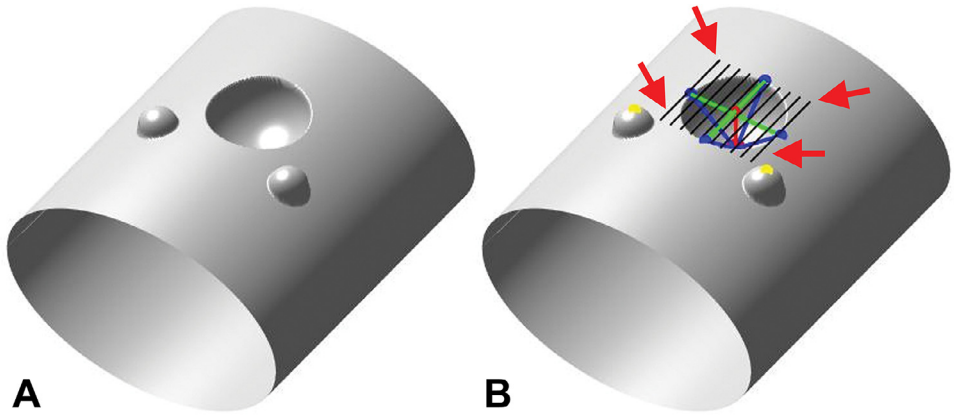

Figure 3. A digital phantom was used to verify the surface analysis tool. (A) The phantom, mimicking pectus excavatum. (B) Analysis results, depicting pectus depth (red), pectus width and length (green), steepness (blue), pectus volume (black) and flaring (yellow) (Color version of figure is available online at http://www.semthorcardiovascsurg.com).

published elsewhere.[10] This protocol ensures standardization of image acquisition. Images were acquired while patients were standing in an upright position, with the hands behind the head and holding breath at end inspiration. A full circumferential 3D image was captured of the patient's torso, including the jugular notch and umbilicus. All images were recorded by a single medical photographer.

Following acquisition, all images were subjected to the developed surface analysis tool. Correctness of the feature identification was assessed and judged by two researchers (NC and JD). In addition, resulting feature values were summarized utilizing the median, interquartile range (IQR) and range.

RESULTS

Analysis Tool Development and Verification

The automatic 3D image surface analysis of pectus excavatum features was developed based on the requirements and methods described. Verification was performed through a digital phantom mimicking the shape of pectus excavatum (Fig. 3B). The pectus volume, width, length and steepness computed by the surface analysis tool demonstrated an absolute error of 4 mm (4%), 2 mm (2%), 12 mL (5%) and 1 degree (3%), respectively. All other calculated features were identical to the predetermined phantom dimensions (ie error: 0%, see Supplementary Material Table 1). Repeated analyses of the digital phantom yielded identical results for all features, both in constant and varying orientations (ie reproducibility of 100%).

Prospective Imaging

Fifty-three consecutive participants presenting with pectus excavatum prospectively received 3D imaging of their chest. One female participant was excluded from analysis due to insufficient scan quality. Of the 52 participants, 46 (88%) were male with an overall median age of 15.3 years (IQR: 14.0–17.7).

Examples of the automatic assessment of pectus excavatum features are shown in Figure 4. The pectus excavatum features were correctly identified for all but one participant. In this one case, flaring was identified without being present (Fig. 5A). Table 1 shows the results of features stratified by gender. Females demonstrated a higher left and right lateral steepness due to the fact that the bilateral points of maximum protrusion were formed by the breasts (see example in Fig. 5B). In addition, for the same reason females demonstrated relatively less pronounced flaring.

The mean duration of analysis per 3D image was 7.6 seconds (standard deviation: 1.0). Key outcomes are summarized in Figure 6.

DISCUSSION

In this study we have developed and verified an innovative and non-invasive surface analysis method that is able to automatically quantify morphological pectus excavatum features based on 3D images. The surface analysis tool demonstrated to be accurate and reproducible, overcoming the limitations of visual assessment and qualitative description of features by surgeons that is prone to inter- and intra-observer variability.[6] It may, moreover, guide and objectify clinical decision making and evaluation of treatments by providing quantitative assessment of the pectus morphology without the exposure to radiation from a CT.

With the automated 3D phenotypical quantification of pectus excavatum features, we aim to overcome the shortcomings of current severity indices, such as the Haller index. This two-dimensional measure is not able to reflect the full three-dimensional extent of the pectus deformity, as demonstrated by the morphological features visualized in Figure 7 and presented Supplementary Material Table 2. Despite all eight patients in Figure 7 having a Haller index between 3.5 and 3.6, their phenotype showed substantial diversity arising from the combination and severity of features present. The combination of features may thus not only better describe the overall pectus

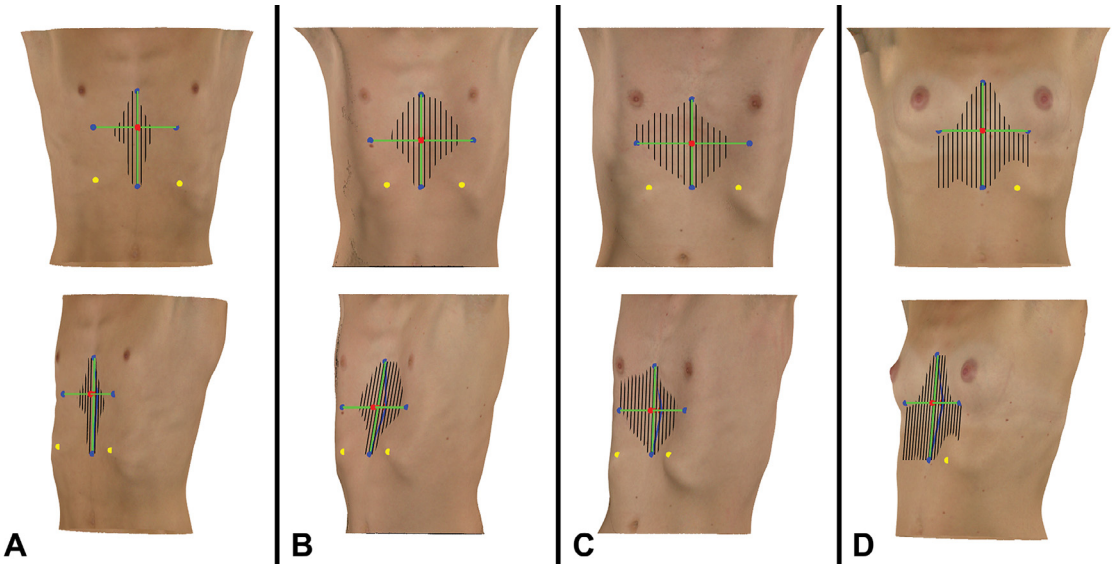

Figure 4. Examples of prospectively imaged patients with pectus excavatum and surface analysis results: pectus depth (red), pectus steepness (blue), pectus width and length (green), pectus volume (black) and flaring (yellow) (Color version of figure is available online at http://www.semthorcardiovascsurg.com).

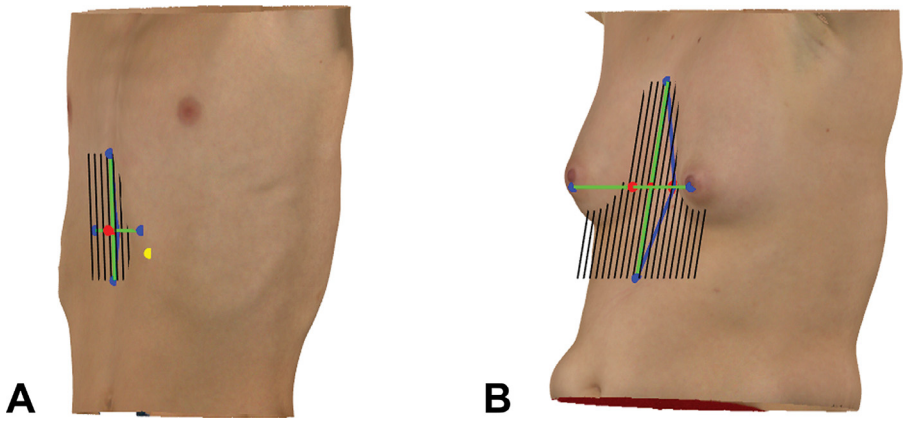

Figure 5. Limitations of the automatic analysis tool that quantifies morphological features of pectus excavatum. (A) In one participant, flaring was identified without being present, while (B) the lateral steepness may be overestimated among females.

morphology, but could in the future also be used to objectify the cosmetic aspects of pectus excavatum and evaluate treatment. Although the proposed features may better define the pectus severity, their clinical value in the process of surgical decision making is yet to be investigated. The three-dimensional surface analysis should be compared to the conventional Haller index which is widely used to help determine indications for corrective surgery.[11] In addition, the morphologic features may serve as a basis for patient-specific models that predict aesthetic outcome or aid in the preoperative planning of surgical treatment.

The surface analysis tool is also able to accurately calculate the external Haller and correction index. Both indices are progressively being investigated as 3D image derived alternatives of the conventional indices to determine severity without exposure to ionizing radiation.[12]

Cartoski et al. [8] and Park et al.[13] both developed a classification of the dysmorphology of pectus excavatum. The classification of Cartoski et al. was developed by categorization of visual pectus excavatum features. Yet, such a classification requires observers to classify the deformity based on visual examination that is prone to inter-observer and intra-observer differences,[6] especially if the deformity is not pronounced or on the border between categories. This disadvantage may be overcome by the developed surface analysis tool that is able to automatically quantify phenotypical pectus excavatum features. Moreover, calculated features may be combined to express specific facets of pectus morphology. For instance, a below-average steepness of the deformity in combination with a larger external Haller index, and/or small mean thoracic area may indicate platythorax. Nonetheless, the classification of different types of deformity based on morphological features requires cut-off

Table 1. Median, Interquartile Range and Absolute Range of Feature Values of 52 Prospectively Imaged Patients With Pectus Excavatum Calculated by the Surface Analysis Tool

	Median (IQR; Absolute range)			
Feature	All (N = 52)	Males (N = 46)	Females (N = 6)	Units
Pectus depth	17 (12–25; 5–46)	18 (12–26; 5–46)	16 (12–20; 10–25)	mm
Pectus width	141 (116–162; 63–194)	142 (115–163; 63–194)	137 (119–152; 80–166)	mm
Pectus length	162 (138–181; 118–228)	162 (138–180; 118–228)	165 (135–195; 122–195)	mm
Pectus volume	68 (27–113; 5–313)	71 (28–115; 5–313)	63 (24–100; 13–200)	mL
Pectus onset position	24 (16–30; 12–36)	24 (17–30; 12–36)	21 (13–29; 13–32)	%
Pectus deepest position	43 (42–46; 29–55)	43 (42–46; 29–55)	45 (42–45; 37–46)	%
Pectus steepness (cranial)	6 (1–9; -15–17)	6 (1–9; -15–17)	5 (-4–7; -8–8)	degrees
Pectus steepness (caudal)	20 (15–27; 5–40)	20 (15–28; 5–40)	24 (16–27; 14–27)	degrees
Pectus steepness (right)	17 (13–23; 2–42)	16 (13–23; 2–42)	18 (13–28; 11–29)	degrees
Pectus steepness (left)	14 (12–21; 4 –35)	14 (12–19; 4–35)	20 (15–26; 10–28)	degrees
Mean cross-sectional area	503 (426–561; 314–811)	508 (429–578; 314–811)	492 (403–516; 357–516)	cm^2
Asymmetry (localized)	0 (-2–2; -17–9)	0 (-2–2; -17–9)	-2 (-3–1; -6–2)	%
Asymmetry (global)	-1 (-2–1; -16–5)	0 (-2–1; -16–5)	-3 (-4–-1; -5–1)	%
Flaring (right)	7 (2–16; -1–26)	8 (3–16; -1–26)	2 (0–10; -1–18)	mm
Flaring (left)	8 (2–14; -6–27)	8 (2–14; -6–27)	5 (1–16; 1–17)	mm

IQR, Interquartile range; N, sample size.

values, which should be subject of future research. It may also be questioned whether a classification yields more clinical value over the separate quantitative values of features, as there may be different levels of severity within a single category (eg, two cup-shaped pectus excavatum may differ in depth). In addition, it may be difficult to categorize deformities if they are less pronounced or borderline.

The feature outcomes differed between males and females; specifically, a higher left and right lateral steepness was found in female patients. This can be attributed to situations where the most excavated point and breasts are at the same transverse level, causing the bilateral steepness to be computed using the breasts as outer maxima of the depression (Fig. 5B). Therefore, in females, the calculated bilateral pectus steepness may be considered as an 'optical' or cosmetic steepness measurement, rather than a clinical steepness. This phenomenon may also occur in adult muscular men, although not observed in the current series wherein patients predominantly encompassed adolescents.

Asymmetry was evaluated both locally and globally. In asymmetric pectus excavatum, the localized level of asymmetry was hypothesized to exceed the global level. Yet, the median

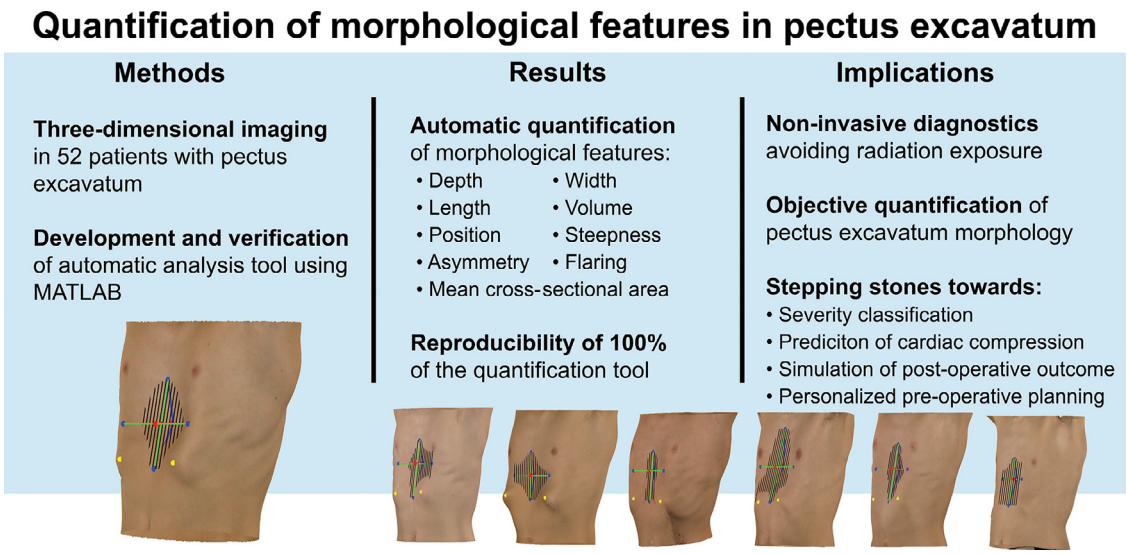

Figure 6. An automatic analysis tool was developed and verified to quantify morphological features of pectus excavatum based on three-dimensional images. Clinical implications include non-invasive and objective diagnostics, while paving a path for various innovative developments to improve clinical care of pectus excavatum.

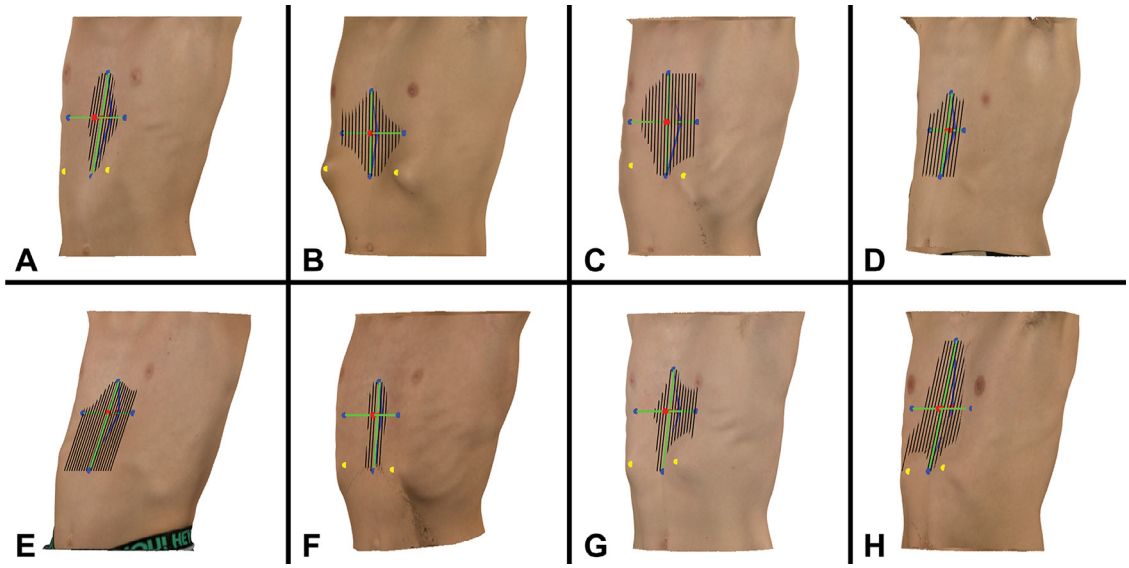

Figure 7. Three-dimensional images of eight patients with pectus excavatum with an equivalent Haller index ranging from 3.5 to 3.6. Visualization of the morphological features highlights the considerable phenotypical heterogeneity despite the comparable Haller index.

asymmetry was found to be comparable (local: 0% versus global: -1%) with an almost perfect correlation coefficient of 0.95. We therefore suggest to only compute the global asymmetry in the future because it provides an overall reflection of asymmetry.

Limitations

Although the developed analysis tool enables quantification of pectus morphology, the findings of this study should be seen in light of some limitations which can be addressed in future research. First of all, evaluation of the clinical feasibility, regarding the correctness of feature identification, was based on the assessment by two researchers. Since there is no gold standard that quantifies morphological features, evaluation of clinical feasibility of the tool was constrained to this subjective assessment. Still, the actual calculations are performed automatically and objectively.

A second limitation relates to the use of ratios to select the region of interest during calculations. To ensure standardization of scan acquisition, the 3D image of the torso includes the jugular notch and umbilicus. The region of interest was defined primarily to focus on the thoracic cage and disregard the abdominal area. The ratios used to define this region have not been clinically validated to accurately define the cranial and caudal boundaries of the thoracic cage, but were evaluated as part of the clinical feasibility assessment.

Furthermore, subsequent images of the same patient may result in different feature values, introduced by the 3D imaging device and patient posture (including differences related to the respiratory phase). Here, an imaging protocol was adopted to ensure standardization of image acquisition, including patient positioning, phase of respiratory cycle (end inspiration) and completeness of the imaged area. A recent study by Daemen et al.[14] demonstrated that when abiding by this imaging protocol, subsequent images obtained by the Artec Leo imaging system provide a clinically acceptable reproducibility of 0.48 mm (standard deviation: 0.60). This reproducibility reflects errors introduced by the scanning device and potential posture changes between subsequent images. Although this study confirmed intra-observer reproducibility, it did not investigate variations introduced by different observers. Nevertheless, all images in this study were obtained by a single photographer, thereby preserving the demonstrated reproducibility. Additionally, we consider that the analysis tool is compatible with images acquired using other devices of comparable scanning resolution (up to 0.20 mm), although this has not been verified here and should be subject of future research.

A digital phantom was chosen to verify the developed analysis tool because its dimensions can be accurately defined with sub-millimeter precision, while errors are likely to be introduced when manufacturing and digitizing a tangible model. Yet, this phantom is a simplified representation of a patient with cup-shaped pectus excavatum. Including other typical pectus and asymmetric shapes may enhance the verification process.

In the verification process, slight errors were observed in the pectus volume, width, length and steepness. These errors are likely to be caused by the fact that slices of 2 mm thickness were used, potentially introducing averaging errors at the excavations' edges.

Additionally, the volume inaccuracy observed was inherent to its method of measurement and the phantoms' design. Because the phantoms' area encircling the pectus depression was posterior to the cranial and caudal surface points, additional volume was included under the vertices of the rectangular plane (Fig. 3B). This is unlikely to occur in clinical 3D

image analyses of cup-shaped pectus excavatum, because the bilateral chest area is typically more exalted compared to the caudal and cranial ends, resulting from the presence of the major pectoral muscles. However, in saucer-like pectus excavatum, where the deformity extends to the lateral sides, an overestimation of the volume may occur. Although a rectangular plane is a simplified representation of a reconstructed chest wall, dynamic models that conform to the surface contour would still introduce errors (eg by disregarding asymmetric deformities). We suggest that a more appropriate method to calculate the pectus volume is based on a valid simulation of the postoperative outcome (ie undeformed shape) of the chest wall, but such a prediction tool is not available yet.

Finally, variations in subcutaneous tissue thickness can influence comparability of morphological measurements between patient groups (eg female versus male and pediatric versus adult) and longitudinal patient observations. However, a typical patient with pectus excavatum is thin,[15] and the shape of the thoracic cage can be adequately represented by the outer body surface. Nevertheless, future research should establish a correction for calculated features based on subcutaneous fat thickness to enhance comparability in a broader population.

Despite these limitations, this study enabled objective and non-invasive quantification of morphologic features of pectus excavatum based on 3D images. The outcomes give rise to new research opportunities, including severity classification, surgical decision-making, prediction of internal anatomy and related abnormalities, simulation of post-operative outcome and personalized pre-operative planning.

CONCLUSION

We have developed and presented an innovative and non-invasive surface analysis tool that is able to automatically quantify morphologic pectus excavatum features based on 3D images. We showed that our analysis tool is accurate, reproducible and feasible in the clinical setting, eliminating the effect of inter- and intra-observer differences. Moreover, morphologic features vary in patients with comparable Haller indices, emphasizing the limitations of the gold standard Haller index and providing an alternative method to describe the full 3D extent of the deformity. Future research should focus on the clinical value of morphologic features in the process of surgical decision-making.

Acknowledgments

The authors would like to gratefully acknowledge Ernst van Loon and Mirianne Curfs-Theunissen, Medical Photographers (Zuyderland Medical Center, Heerlen, The Netherlands), for acquisition of the three-dimensional images.

AUTHOR CONTRIBUTIONS

NC: Conceptualization, methodology, data processing, software, formal analysis, visualization, writing—original draft. JD: Conceptualization, methodology, funding acquisition, formal analysis, writing—original draft. CS: Conceptualization, supervision, writing—review and editing. TL: Formal analysis, visualization, writing—original draft. YV: Conceptualization, methodology, supervision, writing—review and editing. KH: Conceptualization, supervision, writing—review and editing. EdL: Conceptualization, methodology, supervision, writing—review and editing.

INSTITUTIONAL REVIEW BOARD (IRB) APPROVAL

The study was approved by the local ethical committee for scientific research (METC Zuyderland, ID: METCZ20190048, date of approval: April 19, 2019).

INFORMED CONSENT STATEMENT

Written informed consent was obtained prior to inclusion. Additional consent was obtained from the patient's parent(s) or legal guardian if younger than 16 years of age.

SUPPLEMENTARY MATERIAL

Scanning this QR code will take you to the article title page to access supplementary information.

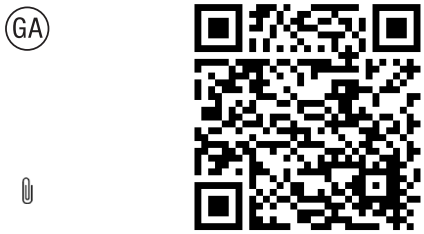

REFERENCES

1. Fokin AA, Steuerwald NM, Ahrens WA, et al: Anatomical, histologic, and genetic characteristics of congenital chest wall deformities. Semin Thorac Cardiovasc Surg 21:44–57, 2009
2. Chung CS, Myrianthopoulos NC: Factors affecting risks of congenital malformations. I. Analysis of epidemiologic factors in congenital malformations. Report from the collaborative perinatal project. Birth Defects Orig Artic Ser 11:1–22, 1975
3. Aloi I, Braguglia A, Inserra A: Pectus excavatum. J Paediatr Child Health 19:S132–S142, 2009
4. Kelly RE Jr: Pectus excavatum: Historical background, clinical picture, preoperative evaluation and criteria for operation. Semin Pediatr Surg 17:181–193, 2008
5. Kelly RE Jr, Quinn A, Varela P, et al: Dysmorphology of chest wall deformities: Frequency distribution of subtypes of typical pectus excavatum and rare subtypes. Arch Bronconeumol 49:196–200, 2013
6. Daemen JHT, de Loos ER, Geraedts TCM, et al: Visual diagnosis of pectus excavatum: An inter-observer and intra-observer agreement analysis. J Ped Surg 2021. https://doi.org/10.1016/j.jpedsurg.2021.06.003. In press
7. Martinez-Ferro M: Indexes for pectus deformities. *Chest wall deformities and corrective procedures*. Springer; 2016, pp 35–60
8. Cartoski MJ, Nuss D, Goretsky MJ, et al: Classification of the dysmorphology of pectus excavatum. J Pediatr Surg 41:1573–1581, 2006
9. Glinkowski W, Sitnik R, Witkowski M, et al: Method of pectus excavatum measurement based on structured light technique. J Biomed Opt 14:044041, 2009

10. Daemen JHT, Loonen TGJ, Coorens NA, et al: Photographic documentation and severity quantification of pectus excavatum through three-dimensional optical surface imaging. J Vis Commun Med 43:190–197, 2020
11. Haller JA Jr., Kramer SS, Lietman SA: Use of ct scans in selection of patients for pectus excavatum surgery: A preliminary report. J Pediatr Surg 22:904–906, 1987
12. Daemen JHT, Loonen TGJ, Lozekoot PWJ, et al: Optical imaging versus ct and plain radiography to quantify pectus severity: A systematic review and meta-analysis. J Thorac Dis 12:1475–1487, 2020
13. Park HJ, Lee SY, Lee CS, et al: The nuss procedure for pectus excavatum: Evolution of techniques and early results on 322 patients. Ann Thorac Surg 77:289–295, 2004
14. Daemen JHT, Loonen TGJ, Verhulst AC, et al: Three-dimensional imaging of the chest wall: A comparison between three different imaging systems. J Surg Res 259:332–341, 2020
15. Pilegaard HK: Growth and pectus excavatum: Is there a relation? Eur J Cardiothorac Surg 50:1110, 2016